Model for cw laser collisionally induced fluorescence in low-temperature discharges

R. S. Stewart, D. J. Smith, I. S. Borthwick,* and A. M. Paterson†
Department of Physics and Applied Physics, John Anderson Building, The University of Strathclyde, 107 Rottenrow, Glasgow G4 ONG, Scotland, United Kingdom

(Received 2 November 1999; revised manuscript received 11 February 2000)

A perturbed steady-state rate-equation model has been developed for the cw laser collisionally induced fluorescence (LCIF) produced by excitation on one of the $1s$-$2p$ noble gas transitions. This work is one part of a wider complementary modeling program which includes cw optogalvanic spectroscopy, optical emission spectroscopy, and optical absorption spectroscopy, with the overall aim of testing all of these models with the same stringently assembled atomic and discharge data set. Our aim here is to demonstrate the principal features of our cw LCIF model by using it to describe our experimental observations produced by pumping transitions originating on the $1s_5$ metastable and $1s_4$ resonance states of neon atoms in the positive column of a normal glow discharge at 2.0 Torr and a discharge current of 5 mA. The model shows that these cw LCIF spectra are dominated by $1s$-$2p$ excitation and electron collisional coupling among the $2p$ states. We show that the model allows us to quantify explicitly the various individual contributions to each line in the cw LCIF spectra. The theory and analyses presented here apply equally well to other noble gases and we believe can be modified appropriately for trace noble gases in atomic-molecular mixtures.

PACS number(s): 52.80.Dy, 52.80.Hc, 52.70.−m

I. INTRODUCTION

Optical diagnostics have become ever more important for the study of a wide range of low-temperature plasmas. Malyshev and Donnelly [1] have shown that for technological plasmas optical actinometry on trace noble gases can be an attractive diagnostic alternative to the Langmuir probe. Also, there have been various comparisons of measurements obtained with electric probes and emission spectroscopy, e.g., Melzer *et al.* [2], while Sugai *et al.* [3] have devised a method whereby optical emission is combined with the electric probe in a biased optical probe technique for obtaining the electron energy distribution. The availability of tunable laser radiation has given access to a number of excited-state perturbation spectroscopies as indicated by the reviews in the recently published book edited by Marcus [4]. We have shown [5] that rigorous analysis of the cw optogalvanic effect (OGE) has potential for obtaining important quantitative information on low-temperature discharges. However, laser-induced fluorescence (LIF) is perhaps the most widely used laser-based diagnostic for low-temperature plasmas. These studies generally investigate the primary LIF (i.e., fluorescence from the pumped level). Such LIF applications in plasmas have been summarized by Zizak *et al.* [6] and recently reviewed by Freegarde and Hancock [7]. The work we discuss here deals with laser collisionally induced fluorescence (LCIF) (i.e., fluorescence from a level which is not pumped directly by the laser). The LCIF technique is a relatively new low-temperature plasma diagnostic. In 1983 Tsuchida *et al.* [8] proposed using LCIF for determining local values of the plasma electron density and since then the technique has been taken up by others. Dubriel and Prigent [9] used it with a pulsed laser to measure the electron density in a low-pressure helium plasma, while Maleki *et al.* [10] observed cw collisionally induced fluorescence in a mercury-argon mixture. More recently the LCIF technique has been further developed [11,12] to obtain the electron temperature as well as the electron density in helium plasmas.

Here we have concentrated on the cw LCIF technique because cw detection is ideal for studying the kinetic behavior of atoms in the highly populated long-lived metastable and resonance states which are so influential to the behavior of low-temperature plasmas. We have developed a perturbed steady-state rate-equation model to describe the collisionally induced spectra resulting from laser perturbation of the $1s$-$2p$ noble gas transitions. Sasso *et al.* [13] have also modeled the cw laser-induced fluorescence spectra which they had observed in the neon positive column. However, they indicated that their model did not give a complete description of the neon cw LCIF observations. Our own previous investigations demonstrated the presence of negative LCIF components [14,15] which clearly could not be explained by coupling of the $2p$ bump (increase in population) alone. Coupling of the hole (decrease in population) created in the lower level is required to explain this phenomenon [15]. In the model we use the results of numerical calculations [16] in which we developed a complete description of the multistep collisional-radiative coupling to determine the laser-induced $1s$ and $2p$ cw perturbations of all excited states included in our model. This account of our cw LCIF model is written with neon in mind but the same discussion applies directly to the other noble gases, argon, krypton, and xenon.

II. EXPERIMENTAL AND THEORETICAL CONSIDERATIONS

Our vacuum and gas handling system has been described elsewhere [17,5]. The system was thoroughly cleaned to

*Present address: Information Systems Engineering, BT, PP 2DAQ, Alexander Bain House, 15 York Street, Glasgow G2 8LA, Scotland, U.K.

†Present address: Applied Materials, Santa Clara, CA.

achieve a base pressure better than 5×10^{-8} Torr before the discharge tube was filled with pure neon to a pressure of 2.0 Torr. For these experiments we deliberately chopped the laser slowly (90 Hz) in order to allow the densities of the excited states of the system to reach their perturbed steady-state values. The fluorescence was recorded using a scanning grating monochromator (Hilger Monospek) followed by a flat-response photomultiplier (Burle C31034A) with lock-in signal detection and computerised recording. Also, in our modeling we wish to apply linearly perturbed steady-state rate equations, hence we reduced the incident power until the induced fluorescence signals were observed to vary linearly with the radiation power absorbed. This allows us to normalize the relevant quantities to the laser pump rate Q, defined as the number of laser photons absorbed in unit time by unit volume of plasma.

III. THE EXCITED-STATE cw PERTURBATIONS

Since we use the results from our numerical modeling [16] for the excited-state cw perturbations, we very briefly recall the relevant fundamentals on which those calculations are based.

In all of our experiments, the laser is tuned to a $1s$-$2p$ transition. The laser-induced perturbations resulting from multiple coupling of the primary laser perturbations were calculated using collisional-radiative branching ratios, and the normalized cw pump rate perturbation was given as the X fraction for each level [17], defined by X_i in

$$\Delta R_i=-X_iQ, \tag{1}$$

where ΔR_i is the cw laser-induced pump rate of level i. The value of X indicates the pump rate perturbation as a fraction of the primary laser pump rate.

In the case of the $1s$ states we showed that, since the total $1s$ depletion coefficients, D_i, are almost entirely independent of the $1s$ densities, by perturbation balance we can write the population perturbations as

$$\Delta N_i=\frac{\Delta R_i}{D_i}=-\frac{X_iQ}{D_i}. \tag{2}$$

We noted previously that evaluation of the $2p$ population perturbations ΔP_i involves accounting for changes induced in their total depletion coefficients as well as in their pump rates. The calculations of ΔP_i are an inherent part of the LCIF model and therefore will be discussed with the model in Sec. IV.

IV. THE cw LCIF MODEL

Throughout the LCIF discussion we will use j and J to label the upper and lower levels ($2p_j$ and $1s_J$) of the LCIF transition under consideration. When considering the LCIF contribution due to the perturbation of a particular level, we will label its population perturbation ΔP_k in the $2p$ case ($k=1$ to 10) and ΔN_K in the case of a $1s$ or the ground state ($K=1$ to 5, $K=1$ for ground).

The aim of our cw LCIF model is to describe the change in emission intensity of a line ($2p_j$-$1s_J$) in the $2p$-$1s$ spectrum resulting from laser perturbation of another of these

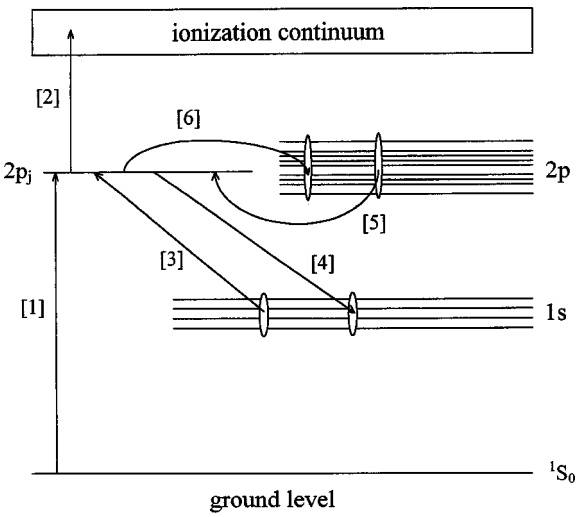

FIG. 1. Processes determining the steady-state $2p_j$ population: (1) Electron collisional excitation from ground, (2) electron collisional ionization from $2p$, (3) electron collisional excitation from $1s$ to $2p$, (4) de-excitation to $1s$ by trapped radiative decay, (5) collisional coupling from other $2p$ states, (6) collisional coupling to other $2p$ states.

transitions. The first step is to write down the steady-state intensity emitted on one of the $2p$-$1s$ transitions. For $2p_j$-$1s_J$ this may be expressed as

$$I_{jJ}=P_jA'_{jJ}, \tag{3}$$

where P_j is the population of level $2p_j$ and A'_{jJ} is the effective Einstein A coefficient. Here we express the relation given for weak radiation trapping by Fujimoto *et al.* [18] in the form

$$A'_{jJ}=\frac{A_{jJ}}{1+\alpha_{jJ}N_J}, \tag{4}$$

where A_{jJ} is the Einstein A coefficients (s^{-1}), α_{jJ} is the trapping coefficient per atom (cm^3), and N_J is the population of $1s_J$ (cm^{-3}).

Using steady-state balance of all of the $2p_j$ processes (Fig. 1) to write the full theoretical expression for I_{jJ} in Eq. (3), we have

$$I_{jJ}=P_jA'_{jJ}=\left\{\frac{n\sum_{K=1}^{5}N_KS_{Kj}+\sum_{k=1}^{10}P_k[nL_{kj}+N_1M_{kj}]}{\sum_{K=2}^{5}\frac{A_{jK}}{(1+\alpha_{jK}N_K)}+\sum_{k=1}^{10}[nL_{jk}+N_1M_{jk}]+nS_j}\right\}\times\frac{A_{jJ}}{1+\alpha_{jJ}N_J}, \tag{5}$$

where n is the electron density (cm^{-3}), N_1 is the ground state density (cm^{-3}), N_{2-5} are the $1s$ level densities (cm^{-3}), S_{1j} are the electron collisional rate coefficients for excitation from the ground state to the $2p$ levels ($cm^3\,s^{-1}$), S_{Kj} for $K=2-5$, are the electron collisional rate coefficients for $1s$ to

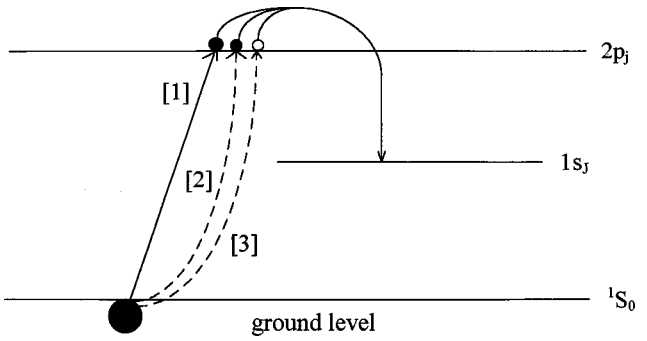

FIG. 2. Laser collisionally induced fluorescence (LCIF) on the $2p_j$-$1s_J$ transition due to the perturbation of the ground state (for the case of positive ΔN_1). (1) Electron collisional excitation of the ground-state perturbation, (2) effect of neutral atom density perturbation on coupling into $2p_j$, (3) effect of neutral atom density perturbation on coupling out of $2p_j$.

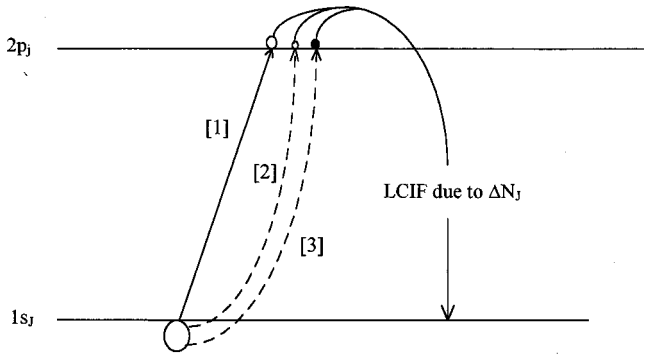

FIG. 3. Laser collisionally induced fluorescence (LCIF) on the $2p_j$-$1s_J$ transition due to the perturbation of a $1s_J$ level (for the case of negative ΔN_J). (1) Coupling of $1s_J$ perturbation into $2p_j$, (2) perturbation of the $2p_j$ depletion coefficient, (3) perturbation of the radiative decay from $2p_j$ to $1s_J$. The equivalent processes of (1) and (2) also occur for the $K \neq J$ case.

$2p$ excitation ($cm^3\,s^{-1}$), L_{kj} are the rate coefficients describing electron-collisional $2p$ mixing ($cm^3\,s^{-1}$), M_{kj} are the ground state atom collisional $2p$ mixing rate coefficients ($cm^3\,s^{-1}$), and S_j are the ionization coefficients from the $2p$ levels ($cm^3\,s^{-1}$).

Clearly the intensity of any $2p$-$1s$ transition is a function of the densities of all of the levels in the system. Since all are perturbed, each will make some contribution to the observed LCIF. We can therefore write the absolute cw laser collisionally induced fluorescence, of the $2p_j$-$1s_J$ transition $\mathcal{F}_{jJ}$, as follows

$$\mathcal{F}_{jJ}=\Delta I_{jJ}=\sum_{K=1}^{5}\frac{\partial I_{jJ}}{\partial N_K}\Delta N_K+\sum_{k=1}^{10}\frac{\partial I_{jJ}}{\partial P_k}\Delta P_k+\mathcal{C}_{jJ}, \quad (6)$$

where $\mathcal{F}_{jJ}$ has units of $cm^{-3}\,s^{-1}$, I_{jJ} is the steady state intensity of the $2p_j$ to $1s_J$ transition ($cm^{-3}\,s^{-1}$), ΔN_1 is the population perturbation of the ground state (cm^{-3}), ΔN_K and ΔP_k are the population perturbations of the $1s_K$ and $2p_k$ levels, respectively (cm^{-3}), and $\mathcal{C}_{jJ}$ is the contribution due to the electric field and electron density perturbations.

A. LCIF due to the ground and 1*s* perturbations

The contributions to the LCIF from the perturbations in the ground and $1s$ states are detailed below. From Eq. (6), the general expression describing the effect of the ground or a $1s$ level population perturbation on the $2p_j$-$1s_J$ LCIF signal is $(\partial I_{jJ}/\partial N_K)\Delta N_K$, where $K=1-5$. There are three distinct ground and $1s$ level contributions to the LCIF. For the transition from the $2p_j$ level down to the $1s_J$ level, these can be separated as follows: (i) $\mathcal{F}_{jJ}$ due to the ground state perturbation ($K=1$), (ii) $\mathcal{F}_{jJ}$ due to the perturbation of a $1s$ level which is not the lower level of the transition ($K \neq J$), (iii) $\mathcal{F}_{jJ}$ due to the perturbation of the $1s$ level on which the transition terminates ($K=J$).

(i) *Ground state*. The LCIF due to the ground state perturbation is illustrated in Fig. 2. The ground perturbation may be positive or negative, depending on the particular laser-perturbed transition. In this illustration we arbitrarily choose the case of a bump.

The ground state contribution to the LCIF arises from coupling of ΔN_1 from the ground to $2p_j$ and from the perturbation of the $2p$ mixing by ground-state atom collisions, into and out of the $2p_j$ level. The ground state perturbation has negligible influence on the LCIF because the large energy separation between the ground and the $2p$ levels means a small excitation coefficient and therefore only weak coupling.

(ii), (iii) *1s levels*. Two cases exist when evaluating the LCIF contribution of a $1s$ level. When considering the effect of the perturbation in a $1s$ level which is not the lower level of the LCIF transition ($K \neq J$), the LCIF is due to the resultant change in the $2p_j$ population. This change in population arises from two sources, (i) coupling of the perturbation from $1s_K$ to $2p_j$ and (ii) perturbation of the depletion coefficient due to the perturbed trapping. We note that a hole in the $1s_K$ population results in both of these contributions being negative, and vice versa in the case of a $1s_K$ bump.

When we consider the effect of the perturbation in the lower level ($1s_J$) of the LCIF transition, as well as the above contributions, we also need to allow for the fact that the effective Einstein A coefficient for that LCIF transition is perturbed. In this case a hole in the $1s_J$ population, as illustrated in Fig. 3, will result in an additional term due to the reduced trapping which contributes an increase in the LCIF signal on the $2p_j$-$1s_J$ transition, and vice versa.

B. LCIF due to the 2*p* perturbations

The total LCIF contribution from the population perturbations of the $2p$ states results from the direct collisional coupling from each of these levels to $2p_j$. To describe this process, we must accurately evaluate ΔP_k, which we noted previously, involves accounting for changes induced in the total depletion coefficient of $2p_k$ as well as in the pump rate. We can express the total population perturbation of level $2p_k$ as

$$\Delta P_k=\frac{\Delta R_k}{D_k}-\frac{R_k\Delta D_k}{D_k^2}, \quad (7)$$

where R_k and D_k represent the pump rate ($cm^{-3}\,s^{-1}$) and depletion coefficient (s^{-1}) of the $2p_k$ level. This becomes,

$$\Delta P_k = -\frac{X_{2p_k} Q}{D_k} + \frac{P_k}{D_k} \sum_{K=2}^{5} \Delta N_K A'_{kK} \frac{\alpha_{kK}}{1+\alpha_{kK} N_K}. \quad (8)$$

We note here that ΔN_K is directly proportional to Q in our linear experimental regime, so ΔP_k varies linearly with Q ensuring that this contribution to the total normalized LCIF signal ($\mathcal{F}^Q_{jJ}$) is also independent of the laser absorption.

C. LCIF due to the electron density and axial electric field perturbations

We consider these together using observations from the optogalvanic effect. From the discharge direct current equation it is straightforward to show that the fractional perturbations in current electron density and axial field are related by

$$\Delta i/i = \Delta n/n + \Delta E/E\,. \quad (9)$$

Here the optogalvanic Δi was measured in the usual way with phase-sensitive detection and ΔE was then deduced from the perturbed circuit equation. The axial field was accurately determined [5] using a pair of identical probes and we obtained the electron density [5] from the measured current and literature values of the electron mobility. The only remaining unknown Δn was then found from Eq. (9).

We used our values of ΔEalong with the data published by Tachibana and Phelps [19] and Peuch and Mizzi [20] as functions of the reduced electric field to determine the resulting perturbations in the ground to $1s$ and $2p$ excitation coefficients. The effects of the normalized electron density and electric field perturbations on one- and two-step excitation of the $2p$ states were included in our LCIF model along with the effects of the laser-induced excited-state perturbations discussed above. Our investigations indicate that any effects on the $1s$-$2p$ reexcitation coefficients, which depend on the temperature of the bulk electrons, are minimal compared with the ground to $1s$ and $2p$ effects.

The key feature of Eq. (9) is that the fractional perturbations in n and E are almost equal ($\Delta i/i$ is small) and are always of opposite sign; therefore, their net effect on the LCIF is only significant for those $2p$ levels for which the coupling from $1s_5$ is weak. A full discussion of the Δn and ΔE perturbations is given elsewhere [16]. Proper allowance for the induced changes in the rate coefficients has been a long-time concern for researchers modeling the optogalvanic effect.

D. Final expression for total LCIF

Collecting all the individual terms together, we obtain an expression for the total $\mathcal{F}_{jJ}$ resulting from the laser illumination

$$\mathcal{F}_{jJ} = \frac{A'_{jJ}}{D_j} Y + \mathcal{C}_{jJ}\,, \quad (10)$$

where Y is given by

$$Y = \left\{ \sum_{K=2}^{5} \Delta N_K \left(nS_{Kj} + P_j A'_{jK} \frac{\alpha_{jK}}{1+\alpha_{jK} N_K} \right) \right\} - \Delta N_J P_j D_j \frac{\alpha_{jJ}}{1+\alpha_{jJ} N_J} + \sum_{k=1}^{10} \Delta P_k [nL_{kj} + N_1 M_{kj}] + \Delta N_1 \left\{ nS_{1j} + \sum_{k=1}^{10} P_k M_{kj} - P_j \sum_{k=1}^{10} M_{jk} \right\}. \quad (11)$$

The above expression is utilized for modeling the experimental LCIF signals. In our fitting, we did not have to concern ourselves with every term described above since many are negligible with respect to processes involving the dominant $1s$ perturbations or, where strong electron-collisional coupling exists, the $2p_i$ bump. While our model does account for all of these lesser terms, it is possible to determine the origin of the major contributions, and express the LCIF in a more manageable form. To illustrate the quantitative understanding that our model can provide, we take the example of a laser transition originating on $1s_5$, where the LCIF transition terminates on one of the other $1s$ levels, in which case Eq. (11) becomes

$$Y = \Delta N_5 \left(nS_{5j} + P_j A'_{j5} \frac{\alpha_{j5}}{1+\alpha_{j5} N_5} \right) + \Delta P_i [nL_{ij} + N_1 M_{ij}]. \quad (12)$$

Similar reductions can be made in describing any LCIF signal resulting from a given $1s$-$2p$ laser transition, when all the major terms have been identified.

V. RESULTS AND DISCUSSION

When testing our model against experimental observation, we ensure that our experiments are conducted in the linear regime, wherein the perturbed effects are directly proportional to the absorbed power. This involves reducing the laser power such that there is low laser absorption. The quantity that we wish to model is the collisionally induced fluorescence normalized to the laser pump rate. In the case of LCIF we represent this quantity as $\mathcal{F}^Q_{jJ}$ for the transition $2p_j$-$1s_J$ and for LIF we use $\mathcal{L}^Q_{iL}$ for the transition from the pumped level $2p_i$ down to $1s_L$.

Additionally, we evaluate the ratio of each LCIF line intensity to a chosen primary LIF line (not the laser transition). We take the ratio $\mathcal{F}^Q_{jJ}/\mathcal{L}^Q_{iL}$ which is an ideal quantity for modeling since it is independent of the absorbed laser power but is a sensitive function of the excited-state kinetics which we wish to study. In this way we are comparing lines dominated by collisional processes with ones dominated by radiative transitions.

We made our theoretical cw LCIF calculations using the same complete atomic and discharge data set which we used in our cw OGE model [5], in our numerical modeling of the cw laser-induced excited-state perturbations [16], and in our optical emission and optical absorption spectroscopy (OES and OAS) models. We kept the rate coefficients constant and equal to their 5 mA values, appropriate to the pR product used in our discharge conditions (neon filling pressure $p = 2$ Torr and tube radius $R = 4.25$ mm). The calculations

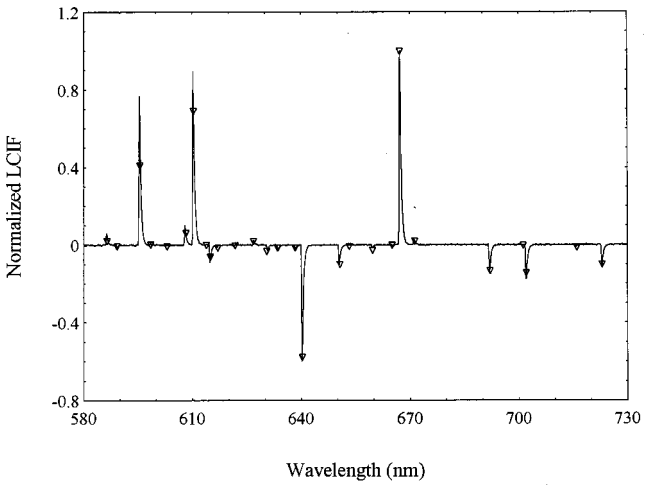

FIG. 4. Laser collisionally induced fluorescence (LCIF) spectrum for $1s_5$-$2p_4$ (594.5 nm) laser transition (the experimental results are given by the solid line, and the triangles represent the predictions of the model).

were carried out using tube-averaged particle densities obtained from measured axial values [21].

Since it is our aim in this discussion to describe the general principles of our cw LCIF model we focus our attention on the cw LCIF spectra produced by tuning the laser to just two $1s$-$2p$ transitions, which is sufficient to explain all of the important features encountered. We present results for the 594.5 nm ($1s_5$-$2p_4$) and 609.6 nm ($1s_4$-$2p_4$) lines. Figures 4 and 5 show that there is excellent agreement between our LCIF model and experiment. Our modeling not only allows an excellent description of the magnitude of the LCIF signal, but can also separate out the individual contributions to the overall signal.

In the case of a standard $1s_5$ pumped line (i.e., one where the upper $2p$ level can radiatively decay down to several of the $1s$ levels), a large hole is created in the $1s_5$ population which, on being mixed around the $1s$ and $2p$ excited states, subsequently dominates the observed LCIF spectrum, and produces a significant number of negative LCIF spectral

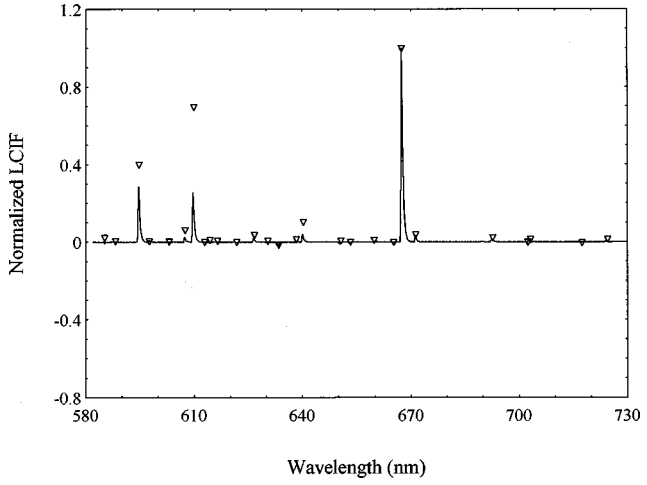

FIG. 5. Laser collisionally-induced fluorescence (LCIF) spectrum for $1s_4$-$2p_4$ (609.6 nm) laser transition (equivalent symbols to those used in Fig. 4).

TABLE I. (a) Influential contributions to $2p_{10}$-$1s_4$ line (724.5 nm) in the LCIF spectrum produced by tuning the laser to 594.5 nm ($1s_5$-$2p_4$). (b) Influential contributions to $2p_{10}$-$1s_5$ line (703.2 nm) in the LCIF spectrum produced by tuning the laser to 594.5 nm ($1s_5$-$2p_4$). (PC refers to perturbation coupling from the $1s_5$ level to the $2p_{10}$, DCP represents the depletion coefficient perturbation term, and T the trapping of the LCIF transition).

(a)	
$1s_5$	−0.089
$1s_5$ (PC)	−0.069
$1s_5$ (DCP)	−0.019
Total	−0.099
(b)	
$1s_5$	−0.121
$1s_5$ (PC)	−0.148
$1s_5$ (DCP)	−0.042
$1s_5$ (T)	0.069
Total	−0.143

lines. However, we still observe some positive LCIF lines (e.g., 585.2, 607.4 nm, Fig. 4), which occur as a result of a combination of strong coupling of the primary $2p$ bump and the fact that a number of the transitions from $1s_5$ to these particular $2p$ levels are forbidden (e.g., $1s_5$-$2p_1$ and $1s_5$-$2p_3$).

Considering first the cw LCIF spectrum resulting from the $1s_5$-$2p_4$ (594.5 nm) laser transition, the dominance of the metastable $1s_5$ hole results in negative LCIF from six of the nine nonpumped levels of which several ($2p_6$,$2p_8$,$2p_9$,$2p_{10}$) exhibit strong signals. These levels are strongly coupled to the $1s_5$ level. By examining particular cw LCIF transitions, we are able to determine the breakdown of the individual contributions to these signals. Table I(a) shows the extent to which the $1s_5$ hole dominates the $2p_{10}$-$1s_4$ LCIF. This transition is ideally described by Eq. (12), which includes the individual and total LCIF due to the key perturbations. We now examine the individual $1s_5$ contributions. Here we are considering the case where $K \neq J$, for which the modeling was discussed in Sec. IV A (ii). For this line Table I(a) shows that coupling of the $1s_5$ hole to the $2p_{10}$ level is the dominant mechanism, although the term arising from perturbation of the depletion coefficient also provides a substantial signal.

Similarly, the typical contributions to cw LCIF terminating on the $1s_5$ level are given by Table I(b). For continuity we have chosen the $2p_{10}$-$1s_5$ transition. Since the $1s_5$ hole is again dominant, here the major contribution is from the $K=J$ case, from Sec. IV A (iii). Coupling of the $1s_5$ hole to the $2p_{10}$ level again provides the most influential constituent, but here the additional $1s_5$ component which arises from the reduced trapping produces a significant contribution of the opposite sign from the other $1s_5$ terms.

For a laser transition originating on one of the resonance levels, for example the 609.6 nm ($1s_4$-$2p_4$) line, we observe distinctly different LCIF spectral characteristics (Fig. 5). In general, such laser transitions result in weaker LCIF signals since the $1s$ perturbations are substantially lower than for a metastable pumped line, and hence their contribution is smaller. Table II(a) illustrates the reduced influence of the $1s$

TABLE II. (a) Individual contributions to $2p_5$-$1s_2$ line (671.7 nm) in the LCIF spectrum produced by tuning the laser to 609.6 nm ($1s_4$-$2p_4$). (b) Individual contributions to $2p_6$-$1s_2$ line (692.9 nm) in the LCIF spectrum produced by tuning the laser to 609.6 nm ($1s_4$-$2p_4$).

(a)	
$1s_2$	0.001
$1s_3$	0.002
$1s_4$	−0.002
$1s_5$	0.002
$2p_4$ (pumped level)	0.030
Total	0.039
(b)	
$1s_4$	−0.005
$1s_5$	0.023
$2p_4$ (pumped level)	0.002
Total	0.024

perturbations, and clearly shows that in such a case the pumped $2p$ level often plays the major role in determining the cw LCIF. This is highlighted by the significant numbers of positive LCIF signals observed in the spectrum of a resonance pumped line, whereas for a metastable pumped line, positive LCIF lines only occur for levels from which $1s_5$ transitions are either very weak or forbidden. There also exist some positive LCIF lines dominated by the coupling of the $1s_5$ bump, and the most important individual contributions for one such example are given in Table II(b). Here the strong coupling of the $1s_5$ perturbation to the $2p_6$ level, combined with weak $2p_4$-$2p_6$ mixing, ensures that, even for resonance level pumping, the long-lived metastable levels can still play a crucial role.

VI. CONCLUSIONS

We present a rate-equation model to describe the cw LCIF in the linearly perturbed regime of the positive column of a normal glow neon discharge. We have shown that our model successfully describes all the different types of spectral features which are observed experimentally when the $1s$ and $2p$ states of neon are linearly perturbed by absorbed tunable laser radiation. As well as predicting the sign and magnitude of the lines observed in the cw LCIF spectrum, the model identifies and quantifies all the sources of the individual contributions to each laser collisionally induced fluorescence line. Although we focus on neon here, our modeling and analysis applies equally well to other noble gases, and we believe, can be modified appropriately for trace noble gases in atomic-molecular mixtures.

ACKNOWLEDGMENTS

The authors wish to thank the Engineering and Physical Sciences Research Council for research funding for this work and for financial support (A.M.P. and D.J.S.).

[1] M. V. Malyshev and V. M. Donnelly, J. Vac. Sci. Technol. A **14**, 1076 (1996).
[2] A. Melzer, R. Flohr, and A. Piel, Plasma Sources Sci. Technol. **4**, 424 (1995).
[3] H. Sugai, H. Toyoda, K. Nakano, and N. Isomura, Plasma Sources Sci. Technol. **4**, 366 (1995).
[4] *Glow Discharge Spectroscopies*, edited by R. K. Marcus (Plenum, New York, 1993).
[5] R. S. Stewart, I. S. Borthwick, D. J. Smith, A. M. Paterson, and C. J. Whitehead, J. Phys. D **33**, 864 (2000).
[6] G. Zizak, N. Omenetto, and J. D. Winefordner, Opt. Eng. (Bellingham) **23**, 749 (1984).
[7] T. G. M. Freegarde and G. Hancock, J. Phys. IV **7**, 15 (1997).
[8] K. Tsuchida, S. Miyake, K. Kadota, and J. Fujita, Plasma Phys. **25**, 991 (1983).
[9] B. Dubreuil and P. Prigent, J. Phys. B **18**, 4597 (1985).
[10] L. Maleki, B. J. Blasenheim, and G. R. Janik, J. Appl. Phys. **68**, 2661 (1990).
[11] E. A. Den Hartog, T. R. O'Brian, and J. E. Lawler, Phys. Rev. Lett. **62**, 1500 (1989).
[12] K. Dzierzega, K. Musiol, E. C. Benck, and J. R. Roberts, J. Appl. Phys. **80**, 3196 (1996).
[13] A. Sasso, M. Ciocca, and E. Arimondo, J. Opt. Soc. Am. B **5**, 1484 (1988).
[14] A. M. Paterson, Ph.D. thesis, Department of Physics and Applied Physics, University of Strathclyde, 1997.
[15] R. S. Stewart, C. J. Whitehead, A. C. Chavez, and I. S. Borthwick (unpublished).
[16] D. J. Smith and R. S. Stewart (unpublished).
[17] R. S. Stewart, K. W. McKnight, and K. I. Hamad, J. Phys. D **23**, 832 (1990).
[18] T. Fujimoto, C. Goto, and K. Fukuda, Phys. Scr. **26**, 443 (1982).
[19] K. Tachibana and A. V. Phelps, Phys. Rev. A **36**, 999 (1987).
[20] V. Peuch and S. Mizzi, J. Phys. D **24**, 1974 (1991).
[21] C. J. Whitehead, Ph.D. thesis, University of Strathclyde, 1992.